Letter

Anisotropy in a wire medium resulting from the rectangularity of a unit cell

Denis Sakhno [1,2,*] Rustam Balafendiev [2,3] and Pavel A. Belov [2,4]

[1]*Qingdao Innovation and Development Center, Harbin Engineering University, Qingdao 266000, Shandong, China*
[2]*School of Physics and Engineering, ITMO University, Kronverksky Prospekt 49, St. Petersburg 197101, Russia*
[3]*Science Institute, University of Iceland, 107 Reykjavik, Iceland*
[4]*School of Engineering, New Uzbekistan University, Movarounnahr Street 1, Tashkent 100000, Uzbekistan*

(Received 15 July 2024; revised 23 September 2024; accepted 25 September 2024; published 7 October 2024)

This study is focused on the dispersion properties of a wire medium formed by a rectangular lattice of parallel wires at frequencies close to its plasma frequency. While the effective medium theory predicts isotropic behavior of transverse magnetic (TM) waves in the structure, numerical simulations reveal noticeable anisotropic properties. This anisotropy is dependent on the lattice rectangularity and reaches over 6% and over 75% along and across the wires respectively for thick wires with radii about 20 times smaller than the smallest period. This conclusion is confirmed by line-of-current approximation theory. The revealed anisotropy effect is observed when the wavelength at the plasma frequency is comparable to the period of the structure. The effect vanishes in the case of extremely thin wires. A dispersion relation for TM waves in the vicinity of the Γ point is obtained in a closed form. This provides an analytical description of the anisotropy effect.

DOI: 10.1103/PhysRevB.110.L140303

Introduction. Metamaterials refer to artificially created media engineered to have some particular properties, which do not appear to be observed in natural materials [1–5]. The variety of their possible applications has been recently raising the interest of researchers to their study [6–10]. Wire media are a class of metamaterials composed of conducting wires periodically arranged in a host material or in a free space [11]. Wire media feature strong spatial dispersion, even at low frequencies [12,13], thus providing subwavelength imaging [14,15] and radiation control [16,17] among other manipulations of electromagnetic fields, which are uncommon [11].

A simple wire medium is formed by parallel metallic wires arranged periodically in a perpendicular plane. Most of the research on this metamaterial [12–19] has been focused on rectangular/square periodicity, that is, an arrangement of the wires of radii r_0 at the nodes of a rectangular lattice having period a in the x direction and period b in the y direction. In the general case a is not equal to b. The geometry of a simple wire medium formed by a rectangular lattice is shown in Fig. 1.

The square-lattice-based metamaterial ($a = b$) has been most amply studied in scholarly literature [20,21] while the rectangular configuration of the metamaterial ($a \neq b$) has rarely been included in its scope except for a recent work [19]. It is, however, noteworthy that the authors of Refs. [12,18] discussed the rectangular lattice of wires and presented an analytical theory of dispersion for the medium. It is based on the above theory that the present study analyzes simple wire media dispersion properties.

The currently reemerging interest in the wire medium with a rectangular lattice results from the prospects of using this metameterial for reconfigurable microwave cavities in the search for dark matter [22]. While wire medium filled cavities have already been analytically investigated for the case of a square lattice [23], this study has not yet been extended to the case that relies on rectangular lattices for tuning, which is partly due to the anisotropy emerging in such systems.

Anisotropy effect observed. We consider a simple wire medium formed by a rectangular lattice with an $a \times b$ unit cell, where b is assumed to be half as large as a. The wires are assumed to be perfectly electrically conducting (PEC) and having radii $r_0 = b/20$. We have performed a numerical simulation by applying the periodic boundary conditions corresponding to the wave vector $\vec{q} = (q_x, q_y, q_z)^T$ for a unit cell in COMSOL MULTIPHYSICS [24]. The isofrequency contours obtained for $q_z = 0$ are plotted in Fig. 2 with solid lines.

Figure 2 shows that the contours cross the q_x and q_y axes in the points having different coordinates d_x and d_y ($d_x \neq d_y$). In other words, the contours arise from the Γ point and are elliptical before the contours reach the edges of the Brillouin zone at $q_x = \pi/a = \pi/2b$. For the obtained contours the ratio of the ellipse's semiaxes d_x/d_y (a contour's *ellipticity*) tends to be ∼1.13 in the vicinity of the Γ point ($\omega = \omega_p + \delta$, $\delta \to 0$).

The electromagnetic anisotropy for a simple wire medium resulting from the periods of the rectangular lattice changing still needs to be discussed. However, an analogous [25] acoustic task for a two-dimensional array of rigid cylinders was reported in Ref. [26], where the anisotropy for an acoustic wave was analytically and numerically shown in the long-wavelength limit.

The observed contour *ellipticity* cannot be described by the dispersion equation derived in Refs. [12,18],

$$q^2 = q_x^2 + q_y^2 + q_z^2 = k^2 - k_p^2, \tag{1}$$

that predicts circular contours regardless of the period ratio a/b. Equation (1) was obtained in Ref. [18] by applying the

*Contact author: denis.sakhno@metalab.ifmo.ru

 ©2024 American Physical Society

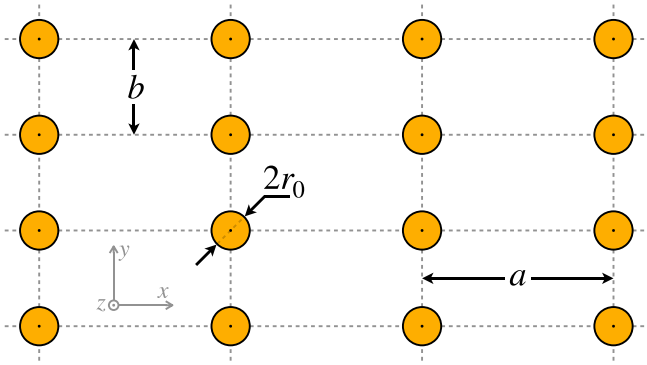

FIG. 1. Geometry of a simple wire metamaterial formed by a rectangular lattice $a \times b$ of parallel wires of radii equal to r_0.

assumption of a small wave number within the metamaterial q ($qa, qb \ll \pi$) and a small vacuum wave number k ($ka, kb \ll \pi$) in *the original (complete) dispersion equation*,

$$F\ \ (\boldsymbol{q}, k, a, b, r_0) = 0, \tag{2}$$

where

$$F(\boldsymbol{q}, k, a, b, r_0) = \frac{1}{\pi} \ln \frac{b}{2\pi r_0} + \frac{1}{k_x^{(0)} b} \frac{\sin k_x^{(0)} a}{\cos k_x^{(0)} a - \cos q_x a} + \sum_{n\neq 0} \left(\frac{1}{k_x^{(n)} b} \frac{\sin k_x^{(n)} a}{\cos k_x^{(n)} a - \cos q_x a} - \frac{1}{2\pi |n|} \right) = 0. \tag{3}$$

In Eq. (3), $k_x^{(n)} = -j\sqrt{(2\pi n/b + q_y)^2 + q_z^2 - k^2}$ and $k = \omega/c$. From now on we will refer to Eq. (1) as a "low-k and q" model. The plasma wave number k_p in this model is expressed as

$$k_p^2 = \frac{2\pi/(ab)}{\log \frac{b}{2\pi r_0} + \sum_{n=1}^{+\infty} \frac{\coth \frac{\pi n a}{b} - 1}{n} + \frac{\pi a}{6b}}. \tag{4}$$

Equation (4) provides an adequate estimation of the plasma frequency even for the thick wires ($b/r_0 = 20$) we used in the simulation above ($\omega_p b/2\pi c \approx 0.190$ vs 0.185 found in COMSOL).

The red dashed lines in Fig. 2 refer to the analytical isofrequency contours calculated using the dispersion Eq. (2). The proper correspondence between the numerical and analytical results (up to the moment when the elliptical contour reaches the edges of the Brillouin zone) confirms the effect of the contour ellipticity and confirms the possibility of using Eq. (2) to explain the elliptical shape of the contours.

We have also verified that a direct numerical solution of the transcendental Eq. (2) matches the results of the computational simulation in COMSOL for the wire media with other ratios $a/b \leqslant 10$ and other wire radii $b/r_0 \geqslant 20$. Based on these results we can suggest that Eq. (2) can be an adequate substitute for the eigenmode solver in COMSOL for a simple wire medium composed of thin wires ($b/r_0 \geqslant 20$) in the vicinity of the Γ point.

Analytical model of anisotropy. In Ref. [18] the low-k and q model [Eq. (1)] was derived from Eq. (2) with the assumption of the parameters being small: (1) $\boldsymbol{q}$ ($qa, qb \ll \pi$) and (2) k ($ka, kb \ll \pi$). However, this derivation is no longer applicable if k is comparable to π/a or π/b. For the example provided in Fig. 2 ($a = 2b$, $b/r_0 = 20$), the wave number k for the first eigenmode of the metamaterial is close to the plasma wave number k_p, which is equal to $0.37\pi/b$, a value comparable to π/b. The low-k and q model not being applicable in this case, another model has to be developed.

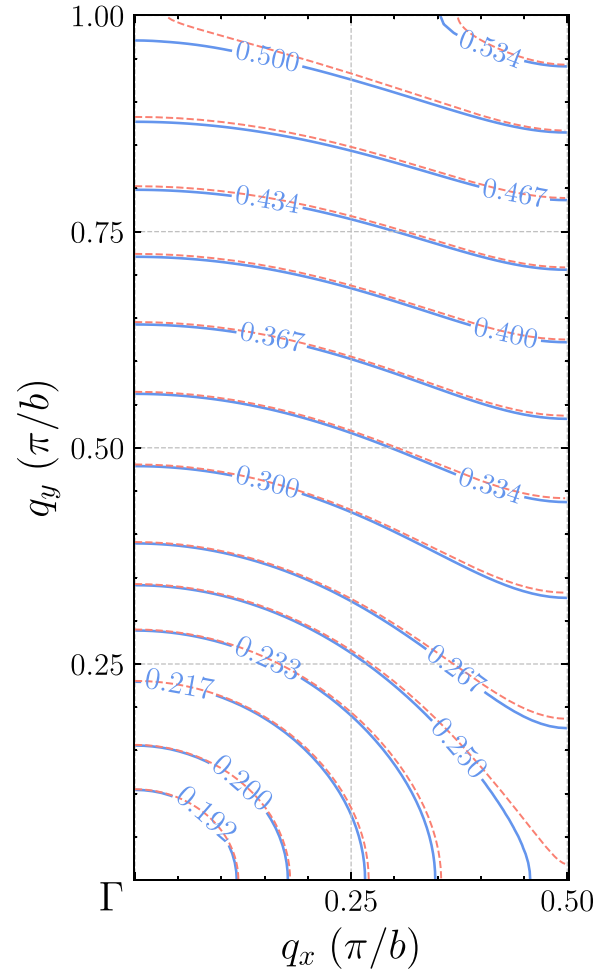

FIG. 2. Isofrequency contours obtained numerically via COMSOL (solid lines) and analytically by solving Eq. (2) (thin dashed lines) for a metamaterial with a rectangular lattice ($a = 2b$). The ratio of the minimal period b to the radii of perfectly conducting wires is $b/r_0 = 20$. Values on isocontours correspond to $\omega b/(2\pi c)$. The plasma frequency for the metamaterial is $\omega_p b/(2\pi c) \approx 0.185$.

We propose to modify the aforementioned model by keeping the assumption about the small q ($qa \ll \pi$ and $qb \ll \pi$) and removing the condition of a small k, thus obtaining *the low-q model*. The expansion of Eq. (2) into a Taylor series up to the second order of small parameters ($q_i a$ and $q_i b$, $i = x, y, z$) results in a more complicated dispersion equation near the Γ point:

$$A(k, a, b)q_x^2 + B(k, a, b)q_y^2 + C(k, a, b)q_z^2 = F_0(k, a, b, r_0). \tag{5}$$

Terms of the first-order and cross terms are equal to zero due to the symmetry of the metamaterial geometry. Equation (5)

divided by function F_0 results in a classical form of a quadric surface:

$$\frac{q_x^2}{d_x^2}+\frac{q_y^2}{d_y^2}+\frac{q_z^2}{d_z^2}=1. \tag{6}$$

The coefficients of q_i^2 $(i=x,y,z)$ are the inverse squares of the ellipsoid semiaxis lengths: $d_x=\sqrt{F_0/A}$, $d_y=\sqrt{F_0/B}$, and $d_z=\sqrt{F_0/C}$.

The coefficients F_0, A, B, and C in Eq. (5) are provided by the following expressions in a closed form,

$$F_0=\frac{1}{\pi}\ln\frac{b}{2\pi r_0}-\frac{1}{kb}\cot\left(\frac{ka}{2}\right)+\frac{1}{\pi}\sum_{n=1}^{\infty}\left[\frac{2\pi\coth\left[\frac{a}{2b}\psi_n(k)\right]}{\psi_n(k)}-\frac{1}{n}\right], \tag{7}$$

$$A=\frac{a^2}{4}\left[\frac{1}{kb}\sin^{-2}\left(\frac{ka}{2}\right)\cot\left(\frac{ka}{2}\right)+2\sum_{n=1}^{\infty}\frac{1}{\psi_n(k)}\frac{\cosh\left[\frac{a}{2b}\psi_n(k)\right]}{\sinh^3\left[\frac{a}{2b}\psi_n(k)\right]}\right], \tag{8}$$

$$B=\frac{a}{2k^2b}\cot\left(\frac{ka}{2}\right)\left[\frac{1}{ka}+\frac{1}{\sin ka}\right]+\sum_{n=1}^{\infty}\frac{b^2}{\psi_n^3(k)}\left(1-\frac{12(\pi n)^2}{\psi_n^2(k)}\right)\coth\left(\frac{a}{2b}\psi_n(k)\right)+\sum_{n=1}^{\infty}\frac{ab/2}{\psi_n^2(k)}\left(1-\frac{12(\pi n)^2}{\psi_n^2(k)}\right)\sinh^{-2}\left(\frac{a}{2b}\psi_n(k)\right)-\sum_{n=1}^{\infty}\frac{2a^2(\pi n)^2}{\psi_n^3(k)}\frac{\cosh\left[\frac{a}{2b}\psi_n(k)\right]}{\sinh^3\left[\frac{a}{2b}\psi_n(k)\right]}, \tag{9}$$

$$C=\frac{a}{2k^2b}\cot\left(\frac{ka}{2}\right)\left[\frac{1}{ka}+\frac{1}{\sin ka}\right]+\sum_{n=1}^{\infty}\frac{b^2}{\psi_n^3(k)}\coth\left(\frac{a}{2b}\psi_n(k)\right)+\sum_{n=1}^{\infty}\frac{ab/2}{\psi_n^2(k)}\sinh^{-2}\left(\frac{a}{2b}\psi_n(k)\right), \tag{10}$$

where $\psi_n(k)=\sqrt{(2\pi n)^2-(kb)^2}$.

Since the system under consideration does not change with the substitutions $q_x\leftrightarrow q_y$ and $a\leftrightarrow b$ performed simultaneously, the following conditions are required for the coefficients:

$$\begin{aligned}A(k,a,b)&=B(k,b,a),\\ C(k,a,b)&=C(k,b,a),\\ F_0(k,a,b,r_0)&=F_0(k,b,a,r_0).\end{aligned} \tag{11}$$

These properties are quite hard to see from expressions (7)–(10), but we have checked them numerically.

Each of the functions F_0, A, B, or C can be calculated for an arbitrary k close to k_p and, hence, isofrequency contours in the low-q model can be plotted without solving Eq. (5) in each point of the mesh $(q_x,q_y,q_z)^T$. On the other hand, to obtain the plasma wave number k_p we have to find the first root of

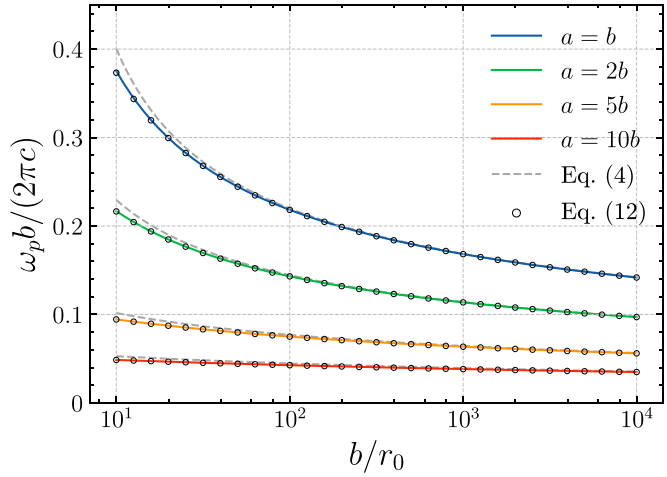

FIG. 3. Plasma frequency (obtained in different ways) dependence on b/r_0 ratios for different a/b values. Solid lines: plasma frequencies calculated via COMSOL; dashed lines: those obtained using Eq. (4). Circle markers were derived using Eq. (12).

the transcendental equation:

$$F_0(k_p,a,b,r_0)=F(k_p,\mathbf{0},a,b,r_0)=0. \tag{12}$$

We also compared the performance of Eqs. (4) and (12) to evaluate the plasma frequency against the numerical results. A plot of plasma frequency dependencies on the b/r_0 ratio for different a/b relations is shown in Fig. 3. The plasma frequency was calculated by three different means: (i) Using COMSOL (the actual plasma frequency), the result is represented by solid lines in the plot; (ii) using Eq. (4), the result is shown in dashed lines; and (iii) using Eq. (12), the result is depicted in circular markers. Equation (12) was shown to perform perfectly: The results of numerical modeling match the analytical results. Hereafter the value of b is maintained fixed to make a unified normalization of all the results.

The greater are the radii of wires r_0, the greater is the deviation of the frequency estimated by Eq. (4) from the actual value obtained in numerical calculations. Table I provides the relative errors of the plasma frequency estimations by Eqs. (4) and (12) for the smallest b/r_0 ratio from Fig. 3 ($b/r_0=10$) and different a/b ratios. It is noteworthy that Eq. (12) provides perfect accuracy of the estimation even for *thick* wires.

Verification of the analytical model. We have compared the metamaterial's anisotropy effects obtained numerically with those described by the low-q model (6) to verify the ability of the analytical model to account for these effects. Figure 4

TABLE I. Relative error ξ of the plasma frequency estimations obtained from Eqs. (4) and (12) for different a/b ratios and the same wire radii $b/r_0=10$.

a/b	$\omega_p^{(\mathrm{num})}b/(2\pi a)$	$\xi^{[\mathrm{Eq.\ (4)}]}$ (%)	$\xi^{[\mathrm{Eq.\ (12)}]}$ (%)
1	0.3753	6.728	0.535
2	0.2168	5.841	0.128
5	0.0944	7.664	0.016
10	0.0486	8.804	0.005

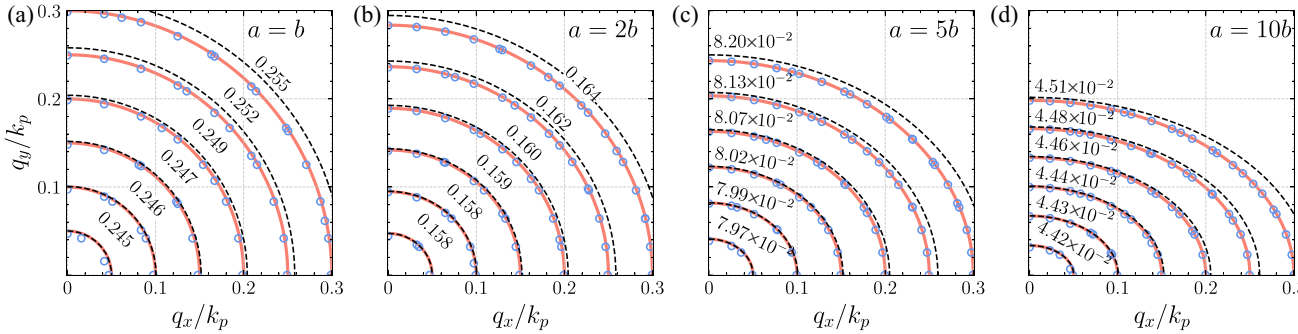

FIG. 4. Isofrequency contours near the Γ point calculated using Eq. (2) (solid lines) and the low-q model [Eq. (5)] (dashed contours) for different geometries of the metamaterial: (a) $a = b$, (b) $a = 2b$, (c) $a = 5b$, and (d) $a = 10b$. For all cases $b/r_0 = 50$ was fixed. The plot axes were normalized by the corresponding k_p: (a) $0.489\pi/b$, (b) $0.315\pi/b$, (c) $0.159\pi/b$, and (d) $0.088\pi/b$. Circle markers indicate the contour points obtained by extracting the contours from numerical simulations.

shows a comparison of the three means of calculating isofrequency contours in the xy plane. The first one is solving the original dispersion Eq. (2) (solid lines in the figure), and the second one uses the low-q model [Eq. (6), plotted by dashed lines]. The third calculation was made using the COMSOL MULTIPHYSICS full-wave simulation [24], and these numerical results are represented by circle markers in the figure. The plots are provided in normalized axes.

The numerical results perfectly match the analytics provided by Eq. (2). Slight inconsistencies of the markers compared to the solid lines are explained by different mesh resolutions that were used for numerical and analytical calculations near the Γ point and by the approximation used for numerical data to obtain contours.

Figure 4 shows that the low-q model diverges from Eq. (2) with an increase in the frequency, while the matching is nearly perfect in the vicinity of the Γ point for every geometry of the metamaterial. Therefore, the proposed model perfectly describes the ellipticity of contours at frequencies slightly greater than the plasma frequency.

To demonstrate the ability of the low-q model (5) to predict the ellipticity of contours for different configurations of the metamaterial, we performed the calculation of d_x/d_y and d_y/d_z ratios for a wide range of geometries (see Fig. 5). The circle markers in Fig. 5 were calculated in Fig. 5(a) as $\sqrt{B/A}$ using expressions (8) and (9) and in Fig. 5(b) as $\sqrt{C/B}$ by calculating the functions (9) and (10). The solid lines in both subfigures were obtained by solving Eq. (2) for fixed k three times: (i) for q_x with fixed $q_y = q_z = 0$, (ii) for q_y with fixed $q_x = q_z = 0$, and (iii) for q_z with fixed $q_x = q_y = 0$ at k near k_p. These two calculations of ellipticity have been shown to perfectly correspond to each other in both planes: xy and yz.

It is important to note that for extremely thin wires ($b/r_0 \to \infty$) the shape of isofrequency contours tends to be circular. This is explained by the plasma frequency decreasing with a decrease of the wire radii (Fig. 3), which makes the low-k and q model applicable because of ka and kb becoming small enough. The higher the a/b ratios, the more difficult it is to achieve a small ka value, hence, the ellipticity for these geometries tends to 1 for very high b/r_0 values.

The results shown in Fig. 5(b) prove to demonstrate the ellipticity even for metamaterials with a square lattice, however, in the yz plane only. The maximum value for the d_y/d_z ratio is equal to ∼1.06. The ellipticity in the xy plane [Fig. 5(a)] achieves a maximal value of ∼1.80 in our simulations for the case of a rectangular lattice with the a/b ratio equal to 10.

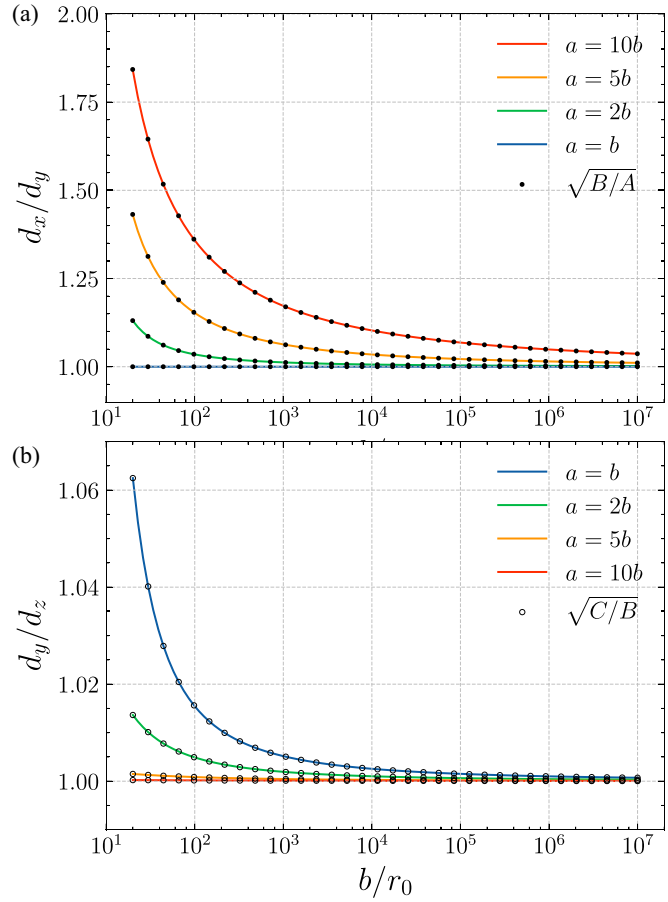

FIG. 5. Dependencies of the ellipticity on the b/r_0 ratio for different a/b values. (a) Solid lines plotted by calculating of q_x/q_y, where q_x and q_y are the solutions of Eq. (2) for fixed k near k_p. Black dots obtained as $\sqrt{B/A}$, where $A(k, a, b)$ and $B(k, a, b)$ are the functions defined in Eqs. (8) and (9). (b) The same comparison between ellipticities in the yz plane obtained via Eq. (2) (solid lines) and by calculating the $C(k, a, b)$ and $B(k, a, b)$ functions (9) and (10) (circle markers).

Conclusion. The present Letter was focused on a simple wire medium formed by a rectangular lattice of parallel wires. The research revealed the anisotropy of transverse magnetic (TM) waves near the Γ point. To describe the anisotropy we proposed and tested the low-q model that is applicable for anisotropy prediction near the Brillouin zone center.

The results of this work are valuable in the context of the axion search, since a simple wire medium has recently served as a basis for axion haloscopes [19,22]. An accurate prediction of the extent of anisotropy in a given rectangular lattice is crucial for the estimation of the tuning ranges for projects on the search for dark matter relying on rectangular wire media for tuning. The tunability of haloscopes is crucial because of the requirement to cover the frequency range not yet studied. Hence, the possibility to employ a rectangular-lattice-based simple wire medium with a precise understanding of anisotropy dependence on the lattice periods paves the way to different opportunities for tuning the haloscope.

Acknowledgment. Numerical simulations of the work were supported by state assignment No. FSER-2024–0041 within the framework of the national project "Science and Universities".

[1] N. Engheta and R. W. Ziolkowski, *Metamaterials: Physics and Engineering Explorations* (Wiley, Hoboken, NJ, 2006).

[2] M. Kadic, G. W. Milton, M. van Hecke, and M. Wegener, 3D metamaterials, Nat. Rev. Phys. **1**, 198 (2019).

[3] A. Alù, N. Engheta, A. Massa, and G. Oliveri, *Metamaterials-by-Design* (Elsevier, Amsterdam, 2024).

[4] K. Sakoda, *Electromagnetic Metamaterials* (Springer, Berlin, 2019).

[5] N. Engheta, Four-dimensional optics using time-varying metamaterials, Science **379**, 1190 (2023).

[6] S. Jahani and Z. Jacob, All-dielectric metamaterials, Nat. Nanotechnol. **11**, 23 (2016).

[7] W. J. Padilla and R. D. Averitt, Imaging with metamaterials, Nat. Rev. Phys. **4**, 85 (2022).

[8] K. Sun, R. Fan, X. Zhang, Z. Zhang, Z. Shi, N. Wang, P. Xie, Z. Wang, G. Fan, H. Liu *et al.*, An overview of metamaterials and their achievements in wireless power transfer, J. Mater. Chem. C **6**, 2925 (2018).

[9] A. O. Krushynska, D. Torrent, A. M. Aragón, R. Ardito, O. R. Bilal, B. Bonello, F. Bosia, Y. Chen, J. Christensen, A. Colombi *et al.*, Emerging topics in nanophononics and elastic, acoustic, and mechanical metamaterials: An overview, Nanophotonics **12**, 659 (2023).

[10] A. Poddubny, I. Iorsh, P. Belov, and Y. Kivshar, Hyperbolic metamaterials, Nat. Photonics **7**, 948 (2013).

[11] C. R. Simovski, P. A. Belov, A. V. Atrashchenko, and Y. S. Kivshar, Wire metamaterials: Physics and applications, Adv. Mater. **24**, 4229 (2012).

[12] P. A. Belov, R. Marques, S. I. Maslovski, I. S. Nefedov, M. Silveirinha, C. R. Simovski, and S. A. Tretyakov, Strong spatial dispersion in wire media in the very large wavelength limit, Phys. Rev. B **67**, 113103 (2003).

[13] C. R. Simovski and P. A. Belov, Low-frequency spatial dispersion in wire media, Phys. Rev. E **70**, 046616 (2004).

[14] P. A. Belov and M. G. Silveirinha, Resolution of subwavelength transmission devices formed by a wire medium, Phys. Rev. E **73**, 056607 (2006).

[15] P. A. Belov, G. K. Palikaras, Y. Zhao, A. Rahman, C. R. Simovski, Y. Hao, and C. Parini, Experimental demonstration of multiwire endoscopes capable of manipulating near-fields with subwavelength resolution, Appl. Phys. Lett. **97**, 191905 (2010).

[16] D. E. Fernandes, S. I. Maslovski, and M. G. Silveirinha, Cherenkov emission in a nanowire material, Phys. Rev. B **85**, 155107 (2012).

[17] M. G. Silveirinha and S. I. Maslovski, Radiation from elementary sources in a uniaxial wire medium, Phys. Rev. B **85**, 155125 (2012).

[18] P. A. Belov, S. A. Tretyakov, and A. Viitanen, Dispersion and reflection properties of artificial media formed by regular lattices of ideally conducting wires, J. Electromagn. Waves. Appl. **16**, 1153 (2002).

[19] N. Kowitt, R. Balafendiev, D. Sun, M. Wooten, A. Droster, M. A. Gorlach, K. van Bibber, and P. A. Belov, Tunable wire metamaterials for an axion haloscope, Phys. Rev. Appl. **20**, 044051 (2023).

[20] J. B. Pendry, A. J. Holden, W. J. Stewart, and I. Youngs, Extremely low frequency plasmons in metallic mesostructures, Phys. Rev. Lett. **76**, 4773 (1996).

[21] J. B. Pendry, A. Holden, D. Robbins, and W. Stewart, Low frequency plasmons in thin-wire structures, J. Phys.: Condens. Matter **10**, 4785 (1998).

[22] A. J. Millar, S. M. Anlage, R. Balafendiev, P. Belov, K. van Bibber, J. Conrad, M. Demarteau, A. Droster, K. Dunne, A. G. Rosso, J. E. Gudmundsson, H. Jackson, G. Kaur, T. Klaesson, N. Kowitt, M. Lawson, A. Leder, A. Miyazaki, S. Morampudi, H. V. Peiris *et al.*, Searching for dark matter with plasma haloscopes, Phys. Rev. D **107**, 055013 (2023).

[23] R. Balafendiev, C. Simovski, A. J. Millar, and P. Belov, Wire metamaterial filled metallic resonators, Phys. Rev. B **106**, 075106 (2022).

[24] COMSOL AB, COMSOL Multiphysics, https://www.comsol.com/.

[25] L. Nicolas, M. Furstoss, and M.-A. Galland, Analogy electromagnetism-acoustics: Validation and application to local impedance active control for sound absorption, Eur. Phys. J.: Appl. Phys. **4**, 95 (1998).

[26] D. Torrent and J. Sánchez-Dehesa, Anisotropic mass density by two-dimensional acoustic metamaterials, New J. Phys. **10**, 023004 (2008).